

Cite this: *RSC Adv.*, 2021, **11**, 11610

Network pharmacology-based analysis for unraveling potential cancer-related molecular targets of Egyptian propolis phytoconstituents accompanied with molecular docking and *in vitro* studies†

Reham S. Ibrahim * and Alaa A. El-Banna

Cancer is one of the predominant causes of death worldwide. The new trend nowadays is to exploit natural products with the hope of developing new anticancer agents with fewer side effects. Propolis is one of these natural products which showed effectiveness in cancer treatment. The aim of this study is to understand the multi-level mechanism of action of propolis constituents in cancer treatment using an integrated approach of network pharmacology-based analysis, molecular docking and *in vitro* cytotoxicity testing. An inhouse database of chemical constituents from Egyptian propolis was compiled and assessed for its ADME properties using the QikProp module in the Schrodinger software. STITCH, UniProt, STRING, KEGG and DAVID databases were used for construction of constituent-target gene, gene-pathway, and constituent-target gene-pathway networks with the aid of Cytoscape 3.8.2. The network pharmacology-based analysis showed that the hit propolis constituents related to cancer targets were genistein, luteolin, benzoic acid, quercetin and vanillic acid, whereas the main cancer-associated targets were CYP1A1, CYP19A1, ESR1, NOS3, CASP3 and AKT1. Twenty-four cancer-related pathways were recognized where the most enriched ones were pathways in cancer and estrogen signaling pathway. The most enriched biological processes involved in the mechanism of action of propolis constituents in cancer treatment were negative regulation of the apoptotic process and the metabolic process and negative regulation of cellular glucuronidation. Molecular docking analysis of the top hit compounds against the most enriched target proteins in the constructed networks was carried out using the Maestro interface of the Schrodinger software. Among hit compounds, quercetin and genistein exhibited the most stabilized interaction. Finally, confirmation of the potential anticancer activity of propolis was assured by *in vitro* cytotoxicity testing of propolis extract on human prostate cancer (DU-145), breast adenocarcinoma (MCF-7) and colorectal adenocarcinoma (Caco-2) cell lines. This study presents deeper insights about propolis molecular mechanisms of action in cancer for the first time using an integrated approach of network pharmacology, molecular docking and *in vitro* testing.

Received 20th February 2021
Accepted 13th March 2021

DOI: 10.1039/d1ra01390d

rsc.li/rsc-advances

1. Introduction

Cancer is among the major causes of death worldwide. It is the second predominant reason for mortality following cardiovascular diseases.¹ It is charged with one in eight deaths in the world, exceeding malaria, AIDS and tuberculosis collectively.² The number of deaths due to cancer in the world is expected to rise from 7.1 million in 2002 to 11.5 million in 2030.³

Many chemotherapeutic agents have been developed during the past five decades. Although these agents were beneficial in the treatment of cancer, they exhibited many adverse side effects.⁴ Therefore, scientific research is needed to improve these agents and develop new ones with no or fewer side effects. Because of this requirement, great attention is now paid to natural products as a promising treasure to discover safer and more effective anticancer agents.

Four categories of natural anticancer agents are marketed today, the vinca alkaloids, the epipodophyllotoxins, the taxanes and the camptothecin derivatives.⁴ Natural products still have great prospect to yield novel anticancer agents and one of these auspicious natural products is propolis.

Propolis is a resinous substance produced by honey bees *via* mixing their salivary and enzymatic secretions with plant sap

Department of Pharmacognosy, Faculty of Pharmacy, Alexandria University, Alexandria, 21521, Egypt. E-mail: rehamsaid84@yahoo.com; reham.abdelkader@alexu.edu.eg; Tel: +201223821098

† Electronic supplementary information (ESI) available. See DOI: [10.1039/d1ra01390d](https://doi.org/10.1039/d1ra01390d)



and gums. It is called “bee glue” because it is used by bees to close up unwanted pores and cracks in their hives. It is also used by bees as an antiseptic to sanitize their hives against microbial infections.⁵ Propolis color and structure vary based on the plant and the geographical origins. It may be green, black, red, white and most commonly brown in color and hard or fragile in structure. There are many botanical origins of propolis, the most commonly identified are chestnut, pine, sweetgum, poplar, oak, birch, elm, coin vine, willow, acacia, eucalyptus, *etc.* The geographical origin includes many countries across the world such as Egypt, China, Thailand, India, Taiwan, Iraq, Greece, Tunisia, Turkey, Cuba, Croatia, Mexico, Portugal, Brazil and Caribbean countries.⁶

From a chemical perspective, the propolis chemome has a remarkable qualitative and quantitative divergence due to specificity of the surrounding flora at the collection site and accordingly geographic, climatic features and harvest seasons. Further, genetic differences among bee races account for this inherent variability, possibly owing to discrete preferences toward appropriate resin sources from various plant families.⁷

Literature survey revealed that propolis is rich in many active constituents mainly polyphenols, flavonoids, amino acids and minerals.⁸ Therefore, it exhibits a variety of health-promoting activities such as antioxidant, antimicrobial, skin emollient, anti-inflammatory, laxative, immunomodulator, antidiabetic, and anticancer activities.⁵ Owing to its positive human health consequences against degenerative diseases,⁹ propolis was recognized as a valuable therapeutic agent and extensively incorporated into commercial health-promoting formulations traditionally consumed worldwide.

The anticancer effect of propolis is its most astounding activity. It is mainly ascribed to its anti-oxidant potential, immune-boosting effect, antiproliferative activity, tumor vascularization inhibition, killing cancer stem cells, alteration of the neoplasm microenvironment, mitigation of chemotherapeutics side effects.¹⁰ Propolis is reported to be effective in the treatment of many types of cancer such as brain and spinal cord, breast, blood, head and neck, skin, pancreas, colon, kidney, liver and bladder cancers.⁶

Comprehension and illustration of the molecular mechanisms by which natural products act on molecular targets is very difficult because of the complex chemome of natural products and the possibility to act synergistically and on multiple targets at the same time. Lately, the explanation of the mechanism of actions of natural products in various diseases with the projection of target genes and pathways have been successfully illustrated by the use of network pharmacology analysis.¹¹⁻¹⁵ This analysis is utilized to construct compound-target-gene-disease network that makes it easy to understand the multi-target mechanism of natural products constituents. Network pharmacology heighten the conception of “network target, multicomponent therapeutics” in a holistic approach comparable to the complexity of natural products metabolomes.¹⁶

The aim of this study is to comprehend the mechanism of the anticancer activity of propolis *via* the network pharmacology analysis. The identification of protein targets and the related pathways followed by gene enrichment analysis were

conducted. Molecular docking analysis was performed on the identified hit compounds mostly related to cancer targets in order to investigate the molecular interactions of these compounds with the target genes. *In vitro* cytotoxicity testing on prostate, breast and colon cancer cell lines was further carried out to prove the potential anticancer activity of Egyptian propolis extract. This study represents deeper insights about propolis molecular mechanisms of action in cancer for the first time using an integrated approach of network pharmacology, molecular docking and *in vitro* testing.

2. Experimental

2.1. Compilation of an in-house database for Egyptian propolis

A database of 100 compounds was compiled from previous literature review on chemical composition of Egyptian propolis (Table S1†). The 2D structures of these compounds were confirmed using ChEMBL (<https://www.ebi.ac.uk/chembl/>) and PubChem (<https://pubchem.ncbi.nlm.nih.gov/>). Then the conversion of these structures to the SMILES format was accomplished using Schrodinger software (2017A).

2.2. ADME and drug-likeness filtration

Filtration of propolis constituents imported from the database was carried out using Qikprop software (Schrodinger suite 2017A) by calculation of absorption, distribution, metabolism, and excretion (ADME) criteria and applying Lipinski's rule of five.¹⁷ In this study, compounds with projected oral bioavailability (OB) of less than 30 were excluded. In addition, compounds that satisfied less than three criteria from Lipinski's rule of five were also excluded.

2.3. Network pharmacology-based analysis

2.3.1. Target genes related to the filtered constituents.

Identification of the target genes related to the filtered constituents was achieved *via* STITCH DB (<http://stitch.embl.de/>, ver. 5.0) with the '*Homo sapiens*' species setting.¹⁸ Genes names, ID, organism and function were retrieved from UniProt (<http://www.uniprot.org/>).^{18,19} Only the '*Homo sapiens*' proteins associated with cancer were retained. Then protein-protein interaction network (PPI network) was constructed using STRING database (<https://string-db.org/>).²⁰

2.3.2. Networks construction and pathway analyses.

Cytoscape 3.8.2 (<http://www.cytoscape.org/>) was utilized to construct three types of networks: constituent-target gene, gene-pathway and constituent-gene-pathway networks in order to investigate the multi-level mechanisms of action of propolis constituents in cancer treatment. In these networks, the nodes represent constituents, genes and pathways, while the edges refer to the interactions between them. The network analyzer plug-in in Cytoscape was utilized to calculate the network parameters. The significance of nodes in each constructed network was assessed using Cytoscape combined score of interactions.

2.3.3. Gene ontology (GO) enrichment analysis of the identified targets.

In order to gain information about gene



ontology and identify the canonical pathways, biological processes, cellular components and molecular functions that were strongly related to the target genes, searching the database for Annotation, Visualization and Integrated Discovery (DAVID) ver. 6.8 (<https://david.ncifcrf.gov/>) and the Kyoto Encyclopedia of Genes and Genomes (KEGG) pathways (<http://www.genome.jp/kegg/pathway.html>) was carried out.^{18–21} Only pathways with *P*-values ≤ 0.01 were chosen.

2.4. Molecular docking studies

The Protein Data Bank (PDB) was used for retrieving the crystal structure of most enriched targets revealed from network pharmacology analysis, which are cytochrome P450 1A1 (6DWN), aromatase (3EQM), estrogen receptor (4J26), endothelial nitric oxide synthase (1M9K), caspase-3 (3DEI) and RAC-alpha serine/threonine-protein kinase (3O96). The selection of crystal structure of each protein was relied on best resolution available. Preparation of the proteins crystallographic structures was accomplished using protein preparation module of Schrodinger's Maestro molecular modeling suit (Schrödinger). Initially, preprocessing of the proteins was carried out by assigning bond orders and hydrogens in addition to creation of zero order bonds to metals and disulphide bonds, all the water molecules exceeding 5 Å from the active site were removed, assignment of hydrogen bonds was performed *via* PROPKA at PH = 7, then energy was minimized using OPLS 3 force field until the relative mean standard deviation (RMSD) of the minimized structure compared to the crystal structure was above 0.30 Å.²² Localization of the binding site for the docking experiments was assigned by the use of receptor grid generation module and the boxes enclosing the centroids of co-crystallized ligands were set as the grids. The compounds 3D structures were imported as SDF file into the LigPrep module of the Maestro molecular modeling package in order to obtain low energy structures of compounds. Adjustment of ionization states was carried out in order to produce all possible states at pH 7. Molecular docking simulations were achieved by the use of Glide docking program of Maestro molecular modeling package implementing extra-precision (XP-Glide) module. The ligand–target interactions including hydrogen bond, ion pair interactions, hydrophobic interactions and the binding modes of the identified compounds were visualized using Maestro interface.

2.5. *In vitro* cytotoxicity assay on human prostate cancer (DU-145), breast adenocarcinoma (MCF-7) and colorectal adenocarcinoma (Caco-2) cell lines

2.5.1. Chemicals and cell lines. Human prostate cancer (DU-145), breast adenocarcinoma (MCF-7) and colorectal adenocarcinoma (Caco-2) cell lines were obtained from Nawah Scientific Inc. (Mokatam, Cairo, Egypt). Dulbecco's Modified Eagle Medium (DMEM), streptomycin, penicillin, fetal bovine serum, sulforhodamine B (SRB) were procured from Lonza (Belgium). Trichloroacetic acid (TCA), acetic acid, TRIS and ethanol were bought from Fisher Scientific, UK. Propolis sample was acquired from reputable bee-keeping communities

from Abees Agricultural Research Unit in Alexandria, Egypt during summer 2020.

2.5.2. Preparation of propolis extract for *in vitro* cytotoxicity assay. A crude sample of propolis was dried and kept overnight at -20°C . The sample was ground *via* manual grinder and then extracted according to the optimized extraction method previously reported in the literature,²³ 2 g of dried powdered sample were extracted using 10 mL of 96% ethanol by sonication in an ultrasonic bath apparatus 28 kHz/1100 W (3 L Alpha Plus, Japan) for 60 min at 35°C . The ethanolic extract was concentrated to dryness under reduced pressure using rotary evaporator at 45°C .

2.5.3. *In vitro* sulforhodamine B (SRB) cytotoxicity assay. Human prostate cancer (DU-145), breast adenocarcinoma (MCF-7) and colorectal adenocarcinoma (Caco-2) cells were separately preserved in Dulbecco's Modified Eagle Media (DMEM) supplied with 100 units per mL of penicillin, 100 mg mL $^{-1}$ of streptomycin, and 10% of heat-inactivated fetal bovine serum in humidified, 5% (v/v) CO $_2$ atmosphere at 37°C . Sulforhodamine B (SRB) assay was applied for assessment of cell viability.^{24,25} Aliquots of 100 μL cell suspension (5×10^3 cells) from each cell line were separately placed in 96-well plates and incubated for 24 h in complete media. Then treatment of the cells with another aliquot of 100 μL media containing propolis at 0.001, 0.01, 0.1, 1, 10, 100 $\mu\text{g mL}^{-1}$ concentrations was carried out. After 72 h exposure to drug, cells were fixed by exchanging media with 150 μL of 10% trichloroacetic acid (TCA) and then the cells were incubated at 4°C for 1 h. The TCA solution was removed, and distilled water was used for washing the cells 5 times. Aliquots of 70 μL SRB solution (0.4% w/v) were added and incubated in a dark place at room temperature for 10 min. Washing the plates 3 times with 1% acetic acid was carried out, then the plates were allowed to air-dry overnight. After that, protein-bound SRB stain was dissolved using 150 μL of TRIS (10 mM); finally, the measurement of the absorbance was performed at 540 nm by the use of a BMG LABTECH® – FLUO star Omega microplate reader (Ortenberg, Germany).

3. Results and discussion

A database of 100 compounds was constructed from previous literature review on chemical composition of Egyptian propolis.

3.1. ADME filtration of propolis constituents

Assessment of the ADME properties of the compounds was carried out *via* QikProp module which measures some physiochemical properties that project the drug-likeness of compounds. These physiochemical properties were summarized by Lipinski's rule of 5. In accordance with Lipinski's rule of 5, a compound of reported biological activity is considered active (having good absorption and/or permeation) if it has lower than ten hydrogen-bond acceptors (Hacc), lower than five hydrogen-bond donors (Hdon), 10 or fewer rotatable bonds (RBN), a molecular weight less than 500 Da and has a calculated log *P* (ClogP) less than five.¹⁷ Only compounds obeying at least three of the above features were retained in the database.



Table 1 Potential protein targets of propolis constituents

Short name of protein	Full name of protein	Interacting compound (s) (combined interaction score)
ABCG2	Broad substrate specificity ATP-binding cassette transporter	Tectochrysin (0.7)
ACSM1	Acyl-CoA synthetase medium-chain family member 1	Benzoic acid (0.952)
ACSM2B	Acyl-CoA synthetase medium-chain family member 2B	Benzoic acid (0.958)
AKT1	RAC-alpha serine/threonine-protein kinase	Genistein (0.96), chrysin (0.7)
ALAD	Delta-aminolevulinic acid dehydratase	Hydroxyvaleric acid (0.949)
AOX1	Aldehyde oxidase 1	Isovanillin (0.861)
AR	Androgen receptor	Genistein (0.959)
ASPA	Aspartoacylase	Triacetin (0.534)
CASP3	Caspase-3	Luteolin (0.947), myricetin (0.733)
CDK1	Cyclin-dependent kinase 1	Apigenin (0.949)
CDK2	Cyclin-dependent kinase 2	Luteolin (0.942)
CES1	Carboxylesterase 1D	Benzoic acid (0.958)
CFTR	Cystic fibrosis transmembrane conductance regulator	Genistein (0.961), gluconate (0.442)
CYP19A1	Aromatase	Genistein (0.962), chrysin (0.931), biochanin A (0.986), apigenin (0.837)
CYP1A1	Cytochrome P450 1A1	Genistein (0.988), galangin (0.981), chrysin (0.841), formononetin (0.722), genkwanin (0.7), ellagic acid (0.444)
CYP1B1	Cytochrome P450 1B1	Quercetin (0.975)
DAO	Diamine oxidase	Benzoic acid (0.993)
EGFR	Epidermal growth factor receptor	Luteolin (0.869)
ESR1	Estrogen receptor alpha	Genistein (0.996), apigenin (0.961), benzoic acid (0.7)
ESR2	Estrogen receptor beta	Genistein (0.996)
F12	Coagulation factor XII	Ellagic acid (0.966)
FOS	Proto-oncogene c-Fos	Luteolin (0.944)
HCK	Tyrosine-protein kinase HCK	Quercetin (0.969)
HRSP12	2-Iminobutanoate/2-iminopropanoate deaminase	Benzoic acid (0.958)
JUN	Transcription factor AP-1	Luteolin (0.946)
MAPK8	Mitogen-activated protein kinase 8	Luteolin (0.951)
MCL1	Induced myeloid leukemia cell differentiation protein	Quercetin (0.987)
MMP9	Matrix metalloproteinase-9	Luteolin (0.949)
NOS3	Nitric oxide synthase	Genistein (0.978), ellagic acid (0.828)
PIK3CG	Phosphatidylinositol 4,5-bisphosphate 3-kinase catalytic subunit gamma isoform	Myricetin (0.928)
PIM1	Serine/threonine-protein kinase pim-1	Quercetin (0.969)
PPARA	Peroxisome proliferator-activated receptor alpha	Naringenin (0.86)
PPARG	Peroxisome proliferator-activated receptor gamma	Genistein (0.964)
PRDX5	Peroxiredoxin-5, mitochondrial	Benzoic acid (0.97)
SIRT1	NAD-dependent protein deacetylase sirtuin-1	Myricetin (0.943)
TMEM37	Transmembrane protein 37	<i>p</i> -Coumaric acid (0.517)
TMEM67	Transmembrane protein 67	Triacetin (0.4)
UGT1A10	UDP glucuronosyltransferase family 1 member A10	Vanillic acid (0.7)
UGT1A3	UDP glucuronosyltransferase family 1 member A3	Vanillic acid (0.7)
UGT1A7	UDP glucuronosyltransferase family 1 member A7	Vanillic acid (0.7)
UGT1A8	UDP glucuronosyltransferase family 1 member A8	Vanillic acid (0.7)

In addition, the oral bioavailability of the gathered compounds was calculated.²⁶ It indicates the extent of the orally administered drug dosage reaching the therapeutic site of action unchanged. Only compounds having OB \geq 30% were

kept in the database. All the compounds of the database (Table S1†) obeyed the specified criteria and thus were retained for further network pharmacology-based analysis.



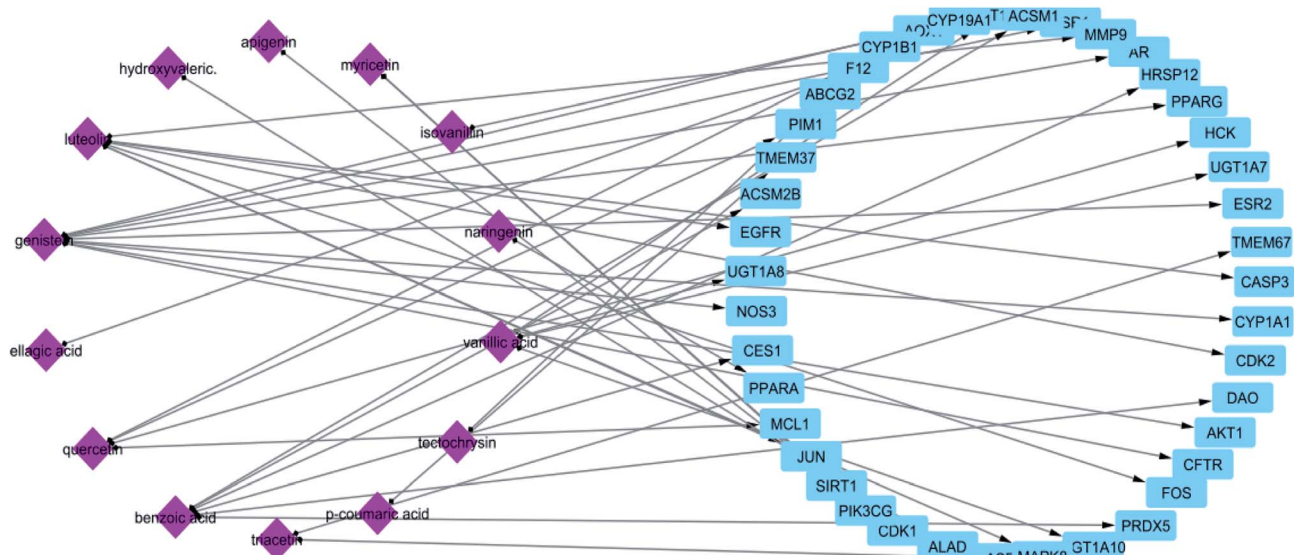


Fig. 1 Network of compound–target gene interactions for propolis constituents by linking 20 compounds and 41 target proteins.

3.2. Identification of cancer-associated target genes of propolis constituents *via* network pharmacology-based analysis

In order to recognize the cancer-associated target genes of propolis compounds, a compound–target network was

constructed using the searching results gained from STITCH 5.0 database. STITCH is a large database that contains information about chemicals interactions. It contains interaction information for more than 68 000 chemicals, including 2200 drugs, and connects them to 1.5 million genes across 373 genomes.²⁷

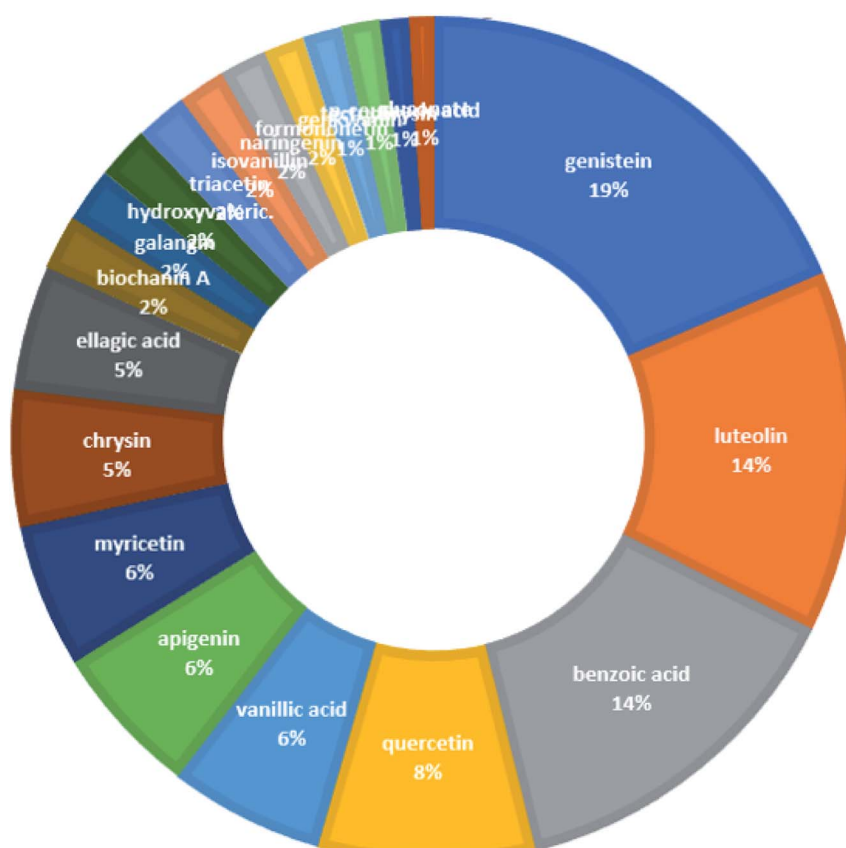


Fig. 2 The distributions % of the compound–target gene (C–T) interactions on the propolis constituents.



UniProt database was utilized to know the role of each identified target gene and its relation to cancer. The Universal Protein Resource (UniProt) is a comprehensive resource for protein sequences and functional annotation, it contains information about more than 550 000 proteins and their functions.²⁸

In STITCH 5.0 database, there are "combined scores" for the interactions between chemicals and genes with stronger interactions exhibiting higher scores. In this study, only compounds having interaction score higher than 0.4 were retained (Table 1). The constructed constituent-target network was composed of 61 nodes (20 constituents and 41 targets) and 55 edges (Fig. 1) with an average of 2.222 targets for each constituent signifying the multi-target feature of the studied compounds.

From the constructed compound–target (C–T) network, it can be shown that the propolis flavonoidal constituents were predominant in the hit list where genistein (flavonoid) exhibited the highest C–T interaction percentage (19%), followed by luteolin (14%) (flavonoid), benzoic acid (14%) (aromatic carboxylic acid), quercetin (8%) (flavonoid), vanillic acid (6%) (phenolic acid), apigenin (6%) (flavonoid), myricetin (6%) (flavonoid), chrysin (5%) (flavonoid) and ellagic acid (5%) (polyphenol) (Fig. 2).

From Fig. 3, it can be concluded that the most enriched cancer-associated target genes which exhibited the highest percentage of interactions with the constituents in this network were CYP1A1 (10%), CYP19A1 (8%), ESR1 (5%), NOS3 (4%),

CASP3 (4%) and AKT1 (4%). These are well-recognized cancer molecular targets where CYP1A1 plays an important role in the metabolism of the polycyclic aromatic hydrocarbons and in the oxidative metabolism of estrogens that might increase the risk of oxidative stress and cancer.²⁹ Also, CYP19A1 (aromatase) plays a critical role in estrogen biosynthesis and thus may be related to the progression of breast cancer and other hormone-dependent cancers.³⁰ In addition, ESR1 is the gene that encodes the estrogen receptor protein. Therefore, plays a role in pathogenesis of cancers.³¹ NOS-3 has also been suggested to modulate different cancer-related events such as angiogenesis, apoptosis, cell cycle, invasion and metastasis.³² Meanwhile, CASP3 is involved in the activation cascade of caspases responsible for apoptosis execution.³³ Whereas, AKT1 regulates many processes including metabolism, proliferation, cell survival, growth and angiogenesis.³⁴ Strong interactions were found between genes in protein–protein network (Fig. 4).

KEGG (Kyoto Encyclopedia of Genes and Genomes) is a database resource for understanding high-level functions and utilities of the biological system from molecular-level information, especially large-scale molecular datasets generated by genome sequencing and other high-throughput experimental technologies.³⁵ KEGG pathways functional enrichment analysis was performed to recognize the signaling pathways and functions of identified target genes (Table 2). From KEGG pathways analysis (Table 2 and Fig. 5), it can be observed that the target

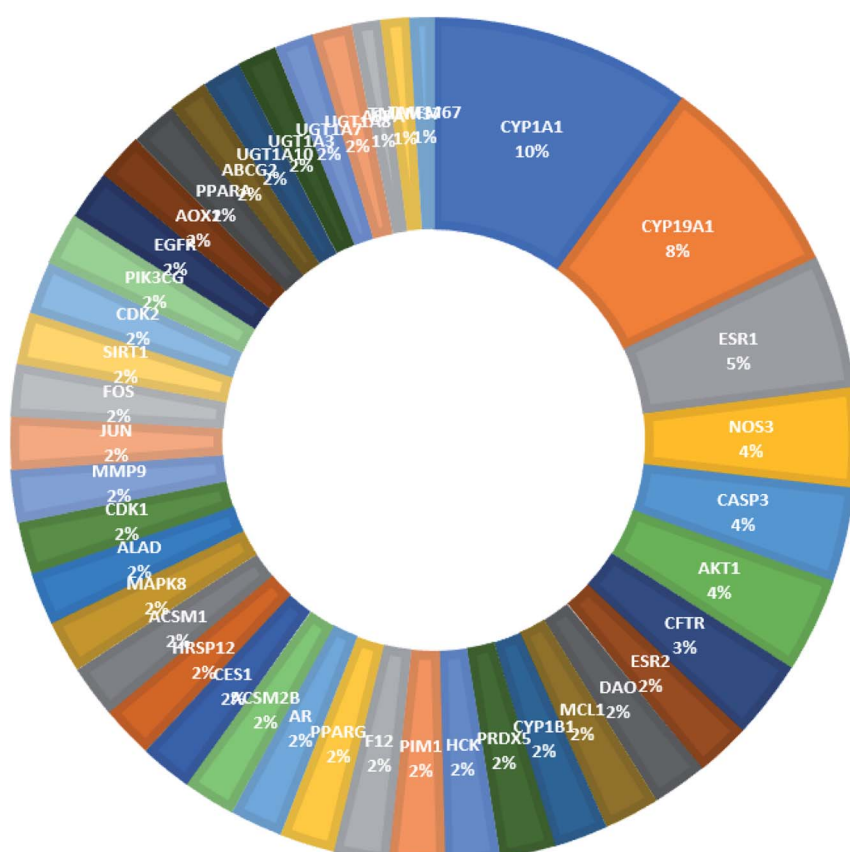


Fig. 3 The distributions % of the compound–target gene (C–T) interactions on the identified cancer-related proteins.



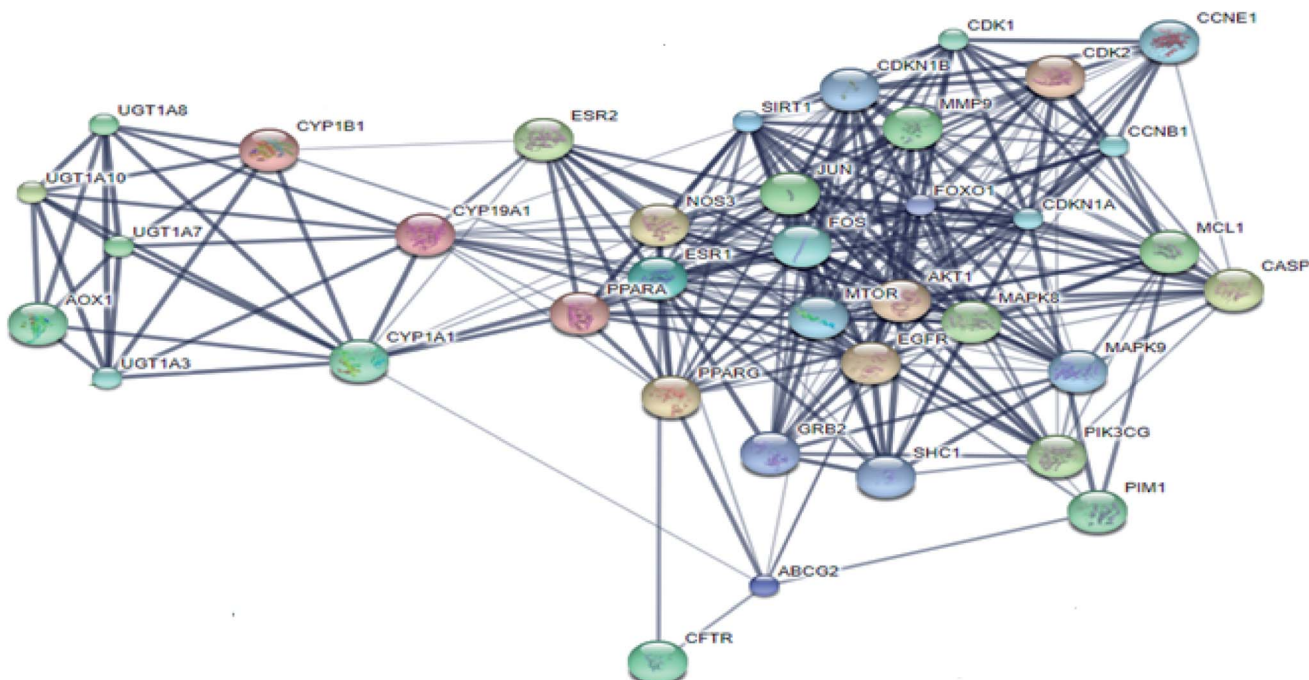


Fig. 4 Protein–protein interaction (PPI) network of identified cancer-related targets.

genes interact with 24 cancer-associated pathways with the most enriched ones were pathways in cancer and estrogen signaling pathway which had the lowest false discovery rate and

the largest number of observed gene count, followed by steroid hormone biosynthesis and microRNAs in cancer.

Merging compound–target and target–pathway networks was carried out to obtain the compound–target–pathway

Table 2 KEGG pathway analysis of potential target genes functions

Pathway ID	Pathway description	Observed gene count	False discovery rate	Matching proteins in network
5200	Pathways in cancer	9	1.09×10^{-13}	AKT1, CASP3, EGFR, FOS, JUN, MAPK8, MMP9, PIK3CG, PPARG
4915	Estrogen signaling pathway	9	5.48×10^{-13}	AKT1, EGFR, ESR1, ESR2, FOS, JUN, MMP9, NOS3, PIK3CG
140	Steroid hormone biosynthesis	7	1.76×10^{-9}	CYP19A1, CYP1A1, CYP1B1, UGT1A10, UGT1A3, UGT1A7, UGT1A8
5206	MicroRNAs in cancer	7	5.94×10^{-9}	CASP3, CYP1B1, EGFR, MCL1, MMP9, PIM1, SIRT1
5205	Proteoglycans in cancer	6	8.09×10^{-8}	AKT1, CASP3, EGFR, ESR1, MMP9, PIK3CG
5210	Colorectal cancer	6	1.33×10^{-7}	AKT1, CASP3, FOS, JUN, MAPK8, PIK3CG
5204	Chemical carcinogenesis	6	3.07×10^{-7}	CYP1A1, CYP1B1, UGT1A10, UGT1A3, UGT1A7, UGT1A8
4010	MAPK signaling pathway	6	2.24×10^{-6}	AKT1, CASP3, EGFR, FOS, JUN, MAPK8
5215	Prostate cancer	5	2.58×10^{-6}	AKT1, AR, EGFR, MMP9, PIK3CG
4151	PI3K-Akt signaling pathway	5	1.58×10^{-5}	AKT1, EGFR, MCL1, NOS3, PIK3CG
5224	Breast cancer	4	1.95×10^{-5}	AKT1, EGFR, ESR1, ESR2
5218	Melanoma	3	0.00014	AKT1, EGFR, PIK3CG
5214	Glioma	3	0.000186	AKT1, EGFR, PIK3CG
5221	Acute myeloid leukemia	3	0.00023	AKT1, PIK3CG, PIM1
5203	Viral carcinogenesis	3	0.000282	CASP3, JUN, PIK3CG
5213	Endometrial cancer	3	0.000318	AKT1, EGFR, PIK3CG
5223	Non-small cell lung cancer	3	0.000511	AKT1, EGFR, PIK3CG
4913	Ovarian steroidogenesis	3	0.000541	CYP19A1, CYP1A1, CYP1B1
5211	Renal cell carcinoma	3	0.000808	AKT1, JUN, PIK3CG
4210	Apoptosis	3	0.000876	AKT1, CASP3, PIK3CG
5202	Transcriptional misregulation in cancer	2	0.00416	MMP9, PPARG
5220	Chronic myeloid leukemia	2	0.00508	AKT1, PIK3CG
5222	Small cell lung cancer	2	0.00701	AKT1, PIK3CG
5219	Bladder cancer	2	0.00877	EGFR, MMP9



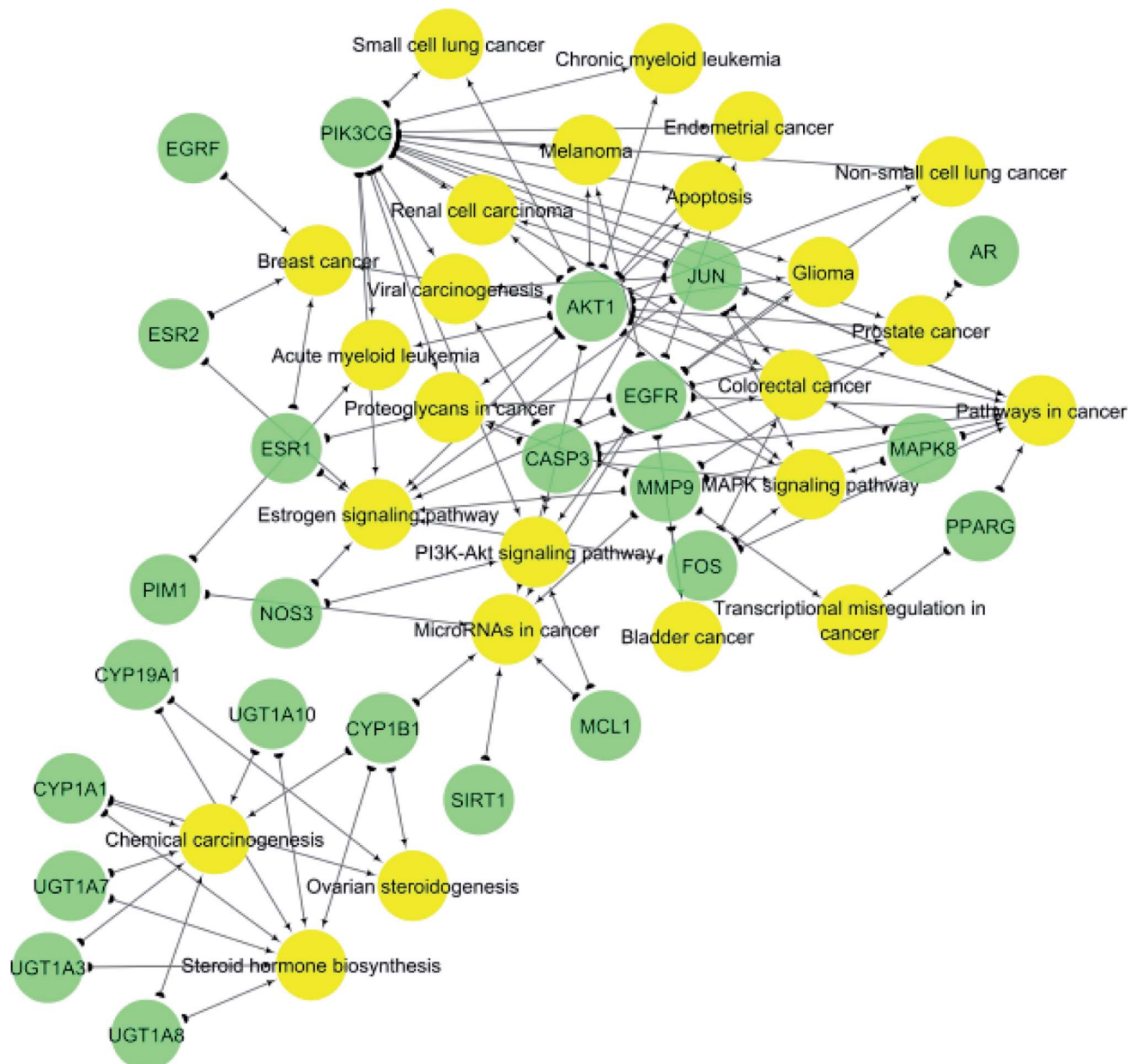


Fig. 5 Gene–pathway network (genes are presented in green color, pathways are presented in yellow color).

network that revealed the multiple interaction nature of the studied propolis constituents together with the identified cancer-associated genes where each node in the network had an average number of interactions of 1.8 (Fig. 6).

In order to validate the results gained from network pharmacology-based analysis, the PubMed was reviewed for studies relating the hit constituents to the different cancer treatment pathways (Table 3). For instance, genistein was found to induce apoptosis in prostate, breast, lung, and pancreas cancer cells by inhibition of NF- κ B and Akt signaling pathways.³⁶ In addition, luteolin was reported to arrest the growth of colon adenocarcinoma cells by inactivation of the PI3K/Akt and ERK1/2 pathways *via* a reduction in insulin-like growth factor-I receptor (IGF-IR) signaling.³⁷ Meanwhile,

benzoic acid derivatives were proved to inhibit murine bladder cancer cells growth and metastasis through inhibition of TNF α /NF κ B and iNOS/NO pathways.³⁸ Moreover, quercetin was declared to suppress the viability and proliferation of breast cancer cells by activation of both apoptosis and necroptosis signaling pathways.³⁹ Also, vanillic acid was proclaimed to inhibit the growth of human colon cancer cells by suppression of hypoxia-inducible factor 1 (HIF-1) expression *via* inhibition of mTOR/p70S6K/4E-BP1 and Raf/MEK/ERK pathways.⁴⁰

3.3. Gene ontology (GO) enrichment analysis for targets

Gene ontology (GO) describes gene products with three independent categories: biological process, cellular component, and



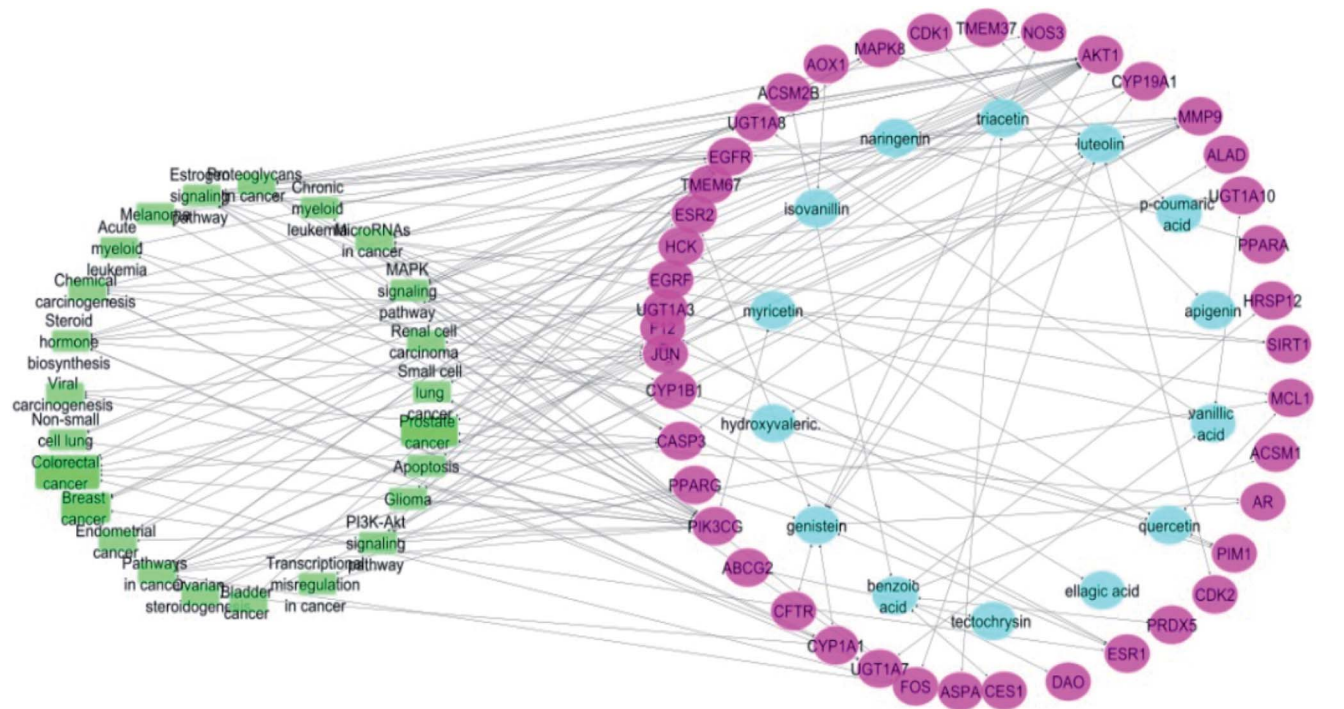


Fig. 6 Compound–target–pathway network (compounds are represented in blue color, targets are presented in pink color and pathways are presented in green color).

molecular function,⁴¹ which may produce multiple GO terms assigned to one query sequence. Gene ontology enrichment analysis of the identified 41 target genes was carried out using DAVID bioinformatics resources with the selection of *Homo sapiens* limit annotation. DAVID is a web-accessible program that combines functional genomic annotations with intuitive graphical summaries. Lists of gene or protein identifiers are rapidly annotated and summarized according to shared categorical data for gene ontology, protein domain, and biochemical pathway membership. DAVID assists in the interpretation of genome-scale datasets by facilitating the transition from data collection to biological meaning.⁴² From Fig. 7A it can be concluded that the most enriched biological processes were negative regulation of apoptotic process, metabolic process and negative regulation of cellular glucuronidation. As shown in Table 3, apoptosis or programmed cell death pathway involved three cancer-associated target genes; AKT1, CASP3 and PIK3CG interacting with propolis compounds. Where, Akt1 is the principal Akt isoform regulating apoptosis in limiting cytokine concentration.⁴³ Caspase-3 is a frequently activated death protease, catalyzing the specific cleavage of many key cellular proteins.⁴⁴ Moreover, inhibition of PIK3CG activation could enhance cancerous cells apoptosis. It is reported that PIK3CG is also a potential target for the treatment of few malignant tumors such as acute lymphoblastic leukemia, medulloblastoma and Kaposi sarcoma.⁴⁵

The most significant molecular functions were enzyme binding, RNA polymerase II transcription factor activity and transcription factor binding. Meanwhile, the most involved

cellular components were cytosol, endoplasmic reticulum membrane and nucleus (Fig. 7A).

Moreover, the GO enrichment analysis using DAVID bioinformatics resources recognized 3 BBID pathways including T-cell receptor and cyclin and p27 cell cycle, 11 BIOCARTA pathways involving inhibition of cellular proliferation, nerve growth factor pathway and TSP-1 induced apoptosis and 28 KEGG pathways including estrogen signaling pathways, colorectal cancer, breast cancer and prostate cancer (Fig. 7B). All recognized pathways possessed *P*-value less than or equal to 0.01.

3.4. Molecular docking studies of hit compounds in the active sites of the most enriched cancer-associated target genes

The Glide module of the Schrodinger suite software was used for calculating the docking XP G scores of propolis hit compounds genistein, luteolin, benzoic acid, quercetin and vanillic acid against the active sites of the most enriched cancer-associated target genes CYP1A1, CYP19A1, ESR1, NOS3, CAPS3 and AKT1. From Table 4, it can be observed that quercetin had the lowest XP G score against cytochrome P450 1A1, estrogen receptor, caspase-3 and RAC-alpha serine/threonine-protein kinase. Whereas, genistein exhibited the most stabilized interaction with aromatase and endothelial nitric oxide synthase.

The 2D and 3D interaction diagrams of quercetin in the active site of cytochrome P450 1A1 (PDB ID 6DWN) (Fig. 8A) revealed the formation of two hydrogen bonds between 3' and 4' hydroxyl groups and Asn222 and a stacking pi-pi interaction between the aromatic ring B of the flavone moiety and Phe224.



Table 3 Summary of literature survey on the top scoring propolis constituents in cancer treatment

Compound	Model	Reference	Mechanism
Genistein	Breast cancer cells (MDA-MB-435 and MDA-MB-231)	PMID: 33249095	Inhibited secreted OPN expression leading to reduced colony formation rate, migration and invasion of MDA-MB-435 and MDA-MB-231 cancer cells. It also activated the MAPK pathway by phosphorylating MEK ¹ and ERK ¹ and increased silent mating type information regulation 2 homolog 1 (SIRT1) expression in these cells
	Breast cancer cells	PMID: 18492603	Inhibited the proto-oncogene HER-2 protein tyrosine phosphorylation
	PC-3 (prostate), MDA-MB-231 (breast), H460 (lung), and BxPC-3 (pancreas) cancer cells	PMID: 16061678	Inhibited the activation of NF-kappaB and Akt signaling pathways that lead to apoptosis
	Human cervical carcinoma cells (HeLa)	PMID: 31766427	Modulated the expression of several genes involved in the cell cycle regulation, migration, inflammation, phosphatidylinositol 3-kinase (PI3K) and mitogen activated kinase-like protein (MAPK) pathway including CCNB1, TWIST1, MMP14, TERT, AKT1, PTPRR, FOS and IL1A
	Human leukemia HL-60 cancer cell	PMID: 30618158	Decreased cell number through G ₂ /M phase arrest and the induction of cell apoptosis through ER stress- and mitochondria-dependent pathways in HL-60 cells
Luteolin	HCT-15 colon adenocarcinoma cell line	PMID: 24099426	Induced growth arrest by inhibiting Wnt/β-catenin/GSK-3β signaling pathway. It also induced apoptosis by caspase-3 mediated manner
	HT-29 colon adenocarcinoma cell line	PMID: 22269172	Downregulated the activation of the PI3K/Akt and ERK1/2 pathways via a reduction in IGF-1R signaling leading to apoptosis
	SW480 and Caco-2 colon cancer cell lines	PMID: 15203384	Induced cell cycle arrest at G2/M phase
	Caco-2 colon cancer cell line	PMID: 20659486	Showed a protective effect against H ₂ O ₂ -induced DNA damage
	Human colon carcinoma cell line Caco-2 (BS TCL 87)	PMID: 26580959	Exerted toxic effects on colon cancer cells by inhibiting both S1P biosynthesis and ceramide traffic
Benzoic acid	Human gastric cancer cell line BGC-823	PMID: 28789432	Induced apoptosis through suppressing the MAPK and PI3K signaling pathways
	MDA-MB-231 breast cancer cells	PMID: 31611756	Induced apoptosis through the caspase cascade and PARP inactivation
	Murine bladder cancer cell line MB49	PMID: 31877271	Benzoic acid derivatives inhibited tumor growth and metastasis through inhibition of TNFα/NFκB and iNOS/NO pathways
	Human cervical carcinoma HeLa cells	PMID: 31366565	Blocked the PI3K, MAPK and WNT pathways by modulating the expression of several proteins leading to the inhibition of cell proliferation, cell cycle arrest, DNA damage and apoptosis in cervical cancer (HeLa) cells
	MCF-7 breast cancer cells	PMID: 28814095	Suppressed viability and proliferation of MCF-7 cells by



Table 3 (Contd.)

Compound	Model	Reference	Mechanism
	Human prostate cancer cell lines (LNCaP, DU-145, and PC-3)	PMID: 29898731	activation of both apoptosis and necroptosis signaling pathways. Apoptosis was induced <i>via</i> increasing expression of Bax and caspase-3 and decreasing expression of Bcl-2 genes. Necroptosis was induced by increasing expression of RIPK1 and RIPK3
	Human pancreatic cancer cell line MIA Paca-2	PMID: 31590760	Exerted its anti-cancer effects by modulating ROS, Akt, and NF- κ B pathways
	AGS human gastric cancer cells	PMID: 30152185	Induced apoptosis and chemosensitivity through RAGE/PI3K/AKT/mTOR pathways
			Induced cell morphological changes and reduced total viability <i>via</i> apoptotic cell death in AGS cells
			Increased reactive oxygen species (ROS) production, decreased the levels of mitochondrial membrane potential, and increased the apoptotic cell number in AGS cells
			Decreased anti-apoptotic protein of Mcl-1, Bcl-2, and Bcl-x but increased pro-apoptotic protein of Bad, Bax, and Bid
			Increased the gene expressions of TNFRSF10D (tumor necrosis factor receptor superfamily, member 10d, decoy with truncated death domain), TP53INP1 (tumor protein p53 inducible nuclear protein 1), and JUNB (jun B proto-oncogene) but decreased the gene expression of VEGFB (vascular endothelial growth factor B), CDK10 (cyclin-dependent kinase 10), and KDELC2 (KDEL [Lys-Asp-Glu-Leu] containing 2) that are associated with apoptosis pathways
Vanillic acid	Human colon cancer HCT116 cells	PMID: 30678221	Suppressed HIF-1 α expression <i>via</i> inhibition of mTOR/p70S6K/4E-BP1 and Raf/MEK/ERK pathways
	Human prostate cancer cell lines (LNCaP, DU145, GM-0637, BPH-1, and TRAMP cell lines)	PMID: 12869308	Vanillic acid methyl ester suppressed Akt/NFKB cell survival signaling pathway therefore it can be used for treatment of prostate cancer
	B16BL6 melanoma cells	PMID: 32722030	Induced STAT3-mediated autophagy to inhibit cancer growth
	benzo(<i>a</i>)pyrene induced lung cancer in Swiss albino mice	PMID: 31468657	It had an efficient preventive action against B(<i>a</i> P-induced lung cancer, and this is attributed to its free-radical scavenging antioxidant activities
	7,12-Dimethylbenz(<i>a</i>)anthracene-induced hamster buccal pouch carcinogenesis	PMID: 30488845	Increased the phase I (cytochrome P450 and cytochrome b5) and decreased phase II (GSH, GR, and DT-diaphorase) detoxification enzymes in DMBA treated hamsters



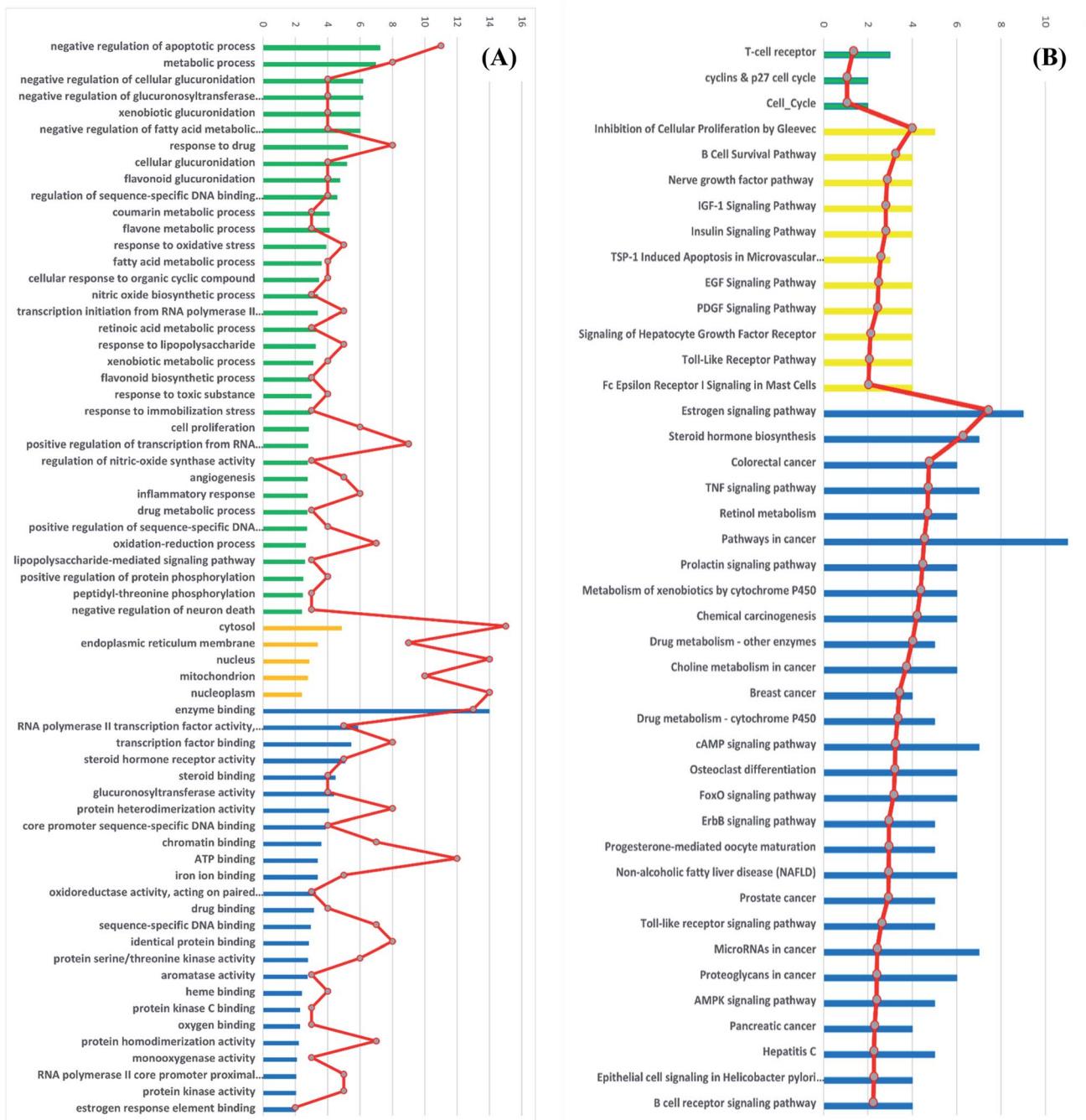


Fig. 7 (A) GO enrichment analysis of identified cancer targets. Biological processes are colored green, cellular components are orange and molecular functions are blue. (B) BBID (green), BIOCARTA (yellow) and KEGG (blue) pathways analysis involved in cancer. The order of importance was ranked by $-\log_{10}(P\text{-value})$ with bar chart. The number of targets stick into each term with line chart.

Table 4 XP G scores of the top hit compounds in the compound–target network against the most enriched cancer-associated target proteins

	Cytochrome P450 1A1 (6DWN)	Aromatase (3EQM)	Estrogen receptor (4J26)	Endothelial nitric oxide synthase (1M9K)	Caspase-3 (3DEI)	RAC-alpha serine/threonine-protein kinase (3O96)
Genistein	-10.968	-9.634	-10.428	-7.951	-7.615	-8.583
Lueolin	-11.551	-8.521	-10.703	-7.107	-6.747	-10.114
Benzoic acid	-5.395	-3.564	-5.646	-7.126	-2.907	-4.194
Quercetin	-11.606	-8.765	-11.074	-7.434	-8.056	-10.452
Vanillic acid	-6.277	-5.170	-7.070	-7.840	-4.466	-5.236



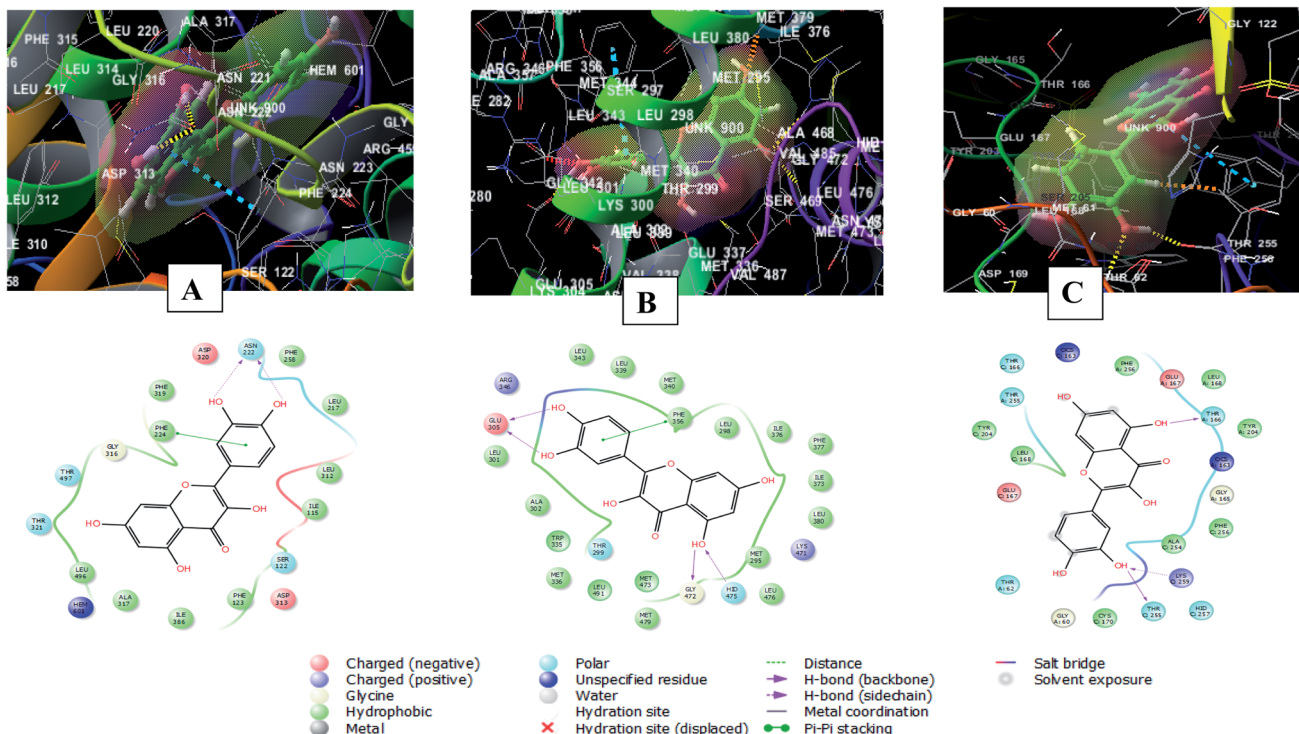


Fig. 8 2D and 3D interaction diagrams of (A) quercetin in the active site of cytochrome P450 1A1 (PDB ID 6DWN) (B) quercetin in the active site of estrogen receptor (PDB ID 4J26) (C) quercetin in the active site of caspase-3 (PDB ID 3DEI).

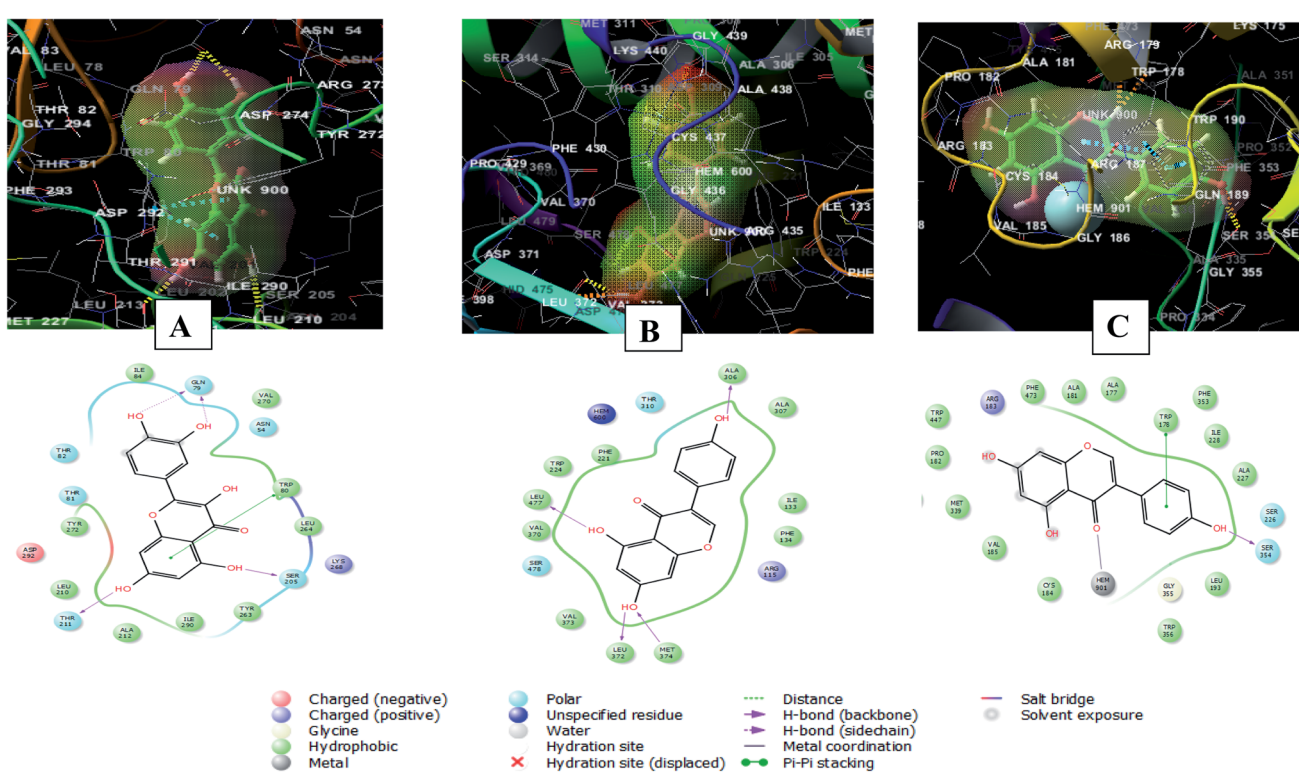


Fig. 9 2D and 3D interaction diagrams of (A) quercetin in the active site of RAC-alpha serine/threonine-protein kinase (PDB ID 3O96) (B) genistein in the active site of aromatase (PDB ID 3EQM) (C) genistein in the active site of endothelial nitric oxide synthase (PDB ID 1M9K).



Charged negative interactions were also observed with Asp313 and Asp320 in addition to hydrophobic interactions with Ile386, Ala317, Leu496, Phe319, Leu217, Phe258, Ile115, Leu312 and Phe123. Moreover, there were polar interactions with Ser122, Thr321 and Thr497.⁴⁶

Meanwhile, the interaction of quercetin with estrogen receptor (PDB ID 4J26) involved four hydrogen bonds between 5, 3', 4' hydroxyl groups and Glu305, Gly472 and His475. In

addition to a stacking pi-pi interaction between the aromatic ring B of the flavone moiety and Phe356. There were also hydrophobic interactions with Met336, Trp335, Met340, Leu339, Leu343, Leu 301, Ala302, Leu 298, Ile376, Leu380, Ile373, Phe377, Met295 and Leu476⁴⁷ (Fig. 8B).

Furthermore, quercetin interacted with caspase-3 (PDB ID 3DEI) using three hydrogen bonds between 3' and 5 hydroxyl groups and Thr255, Lys259 and Thr166. In addition to polar

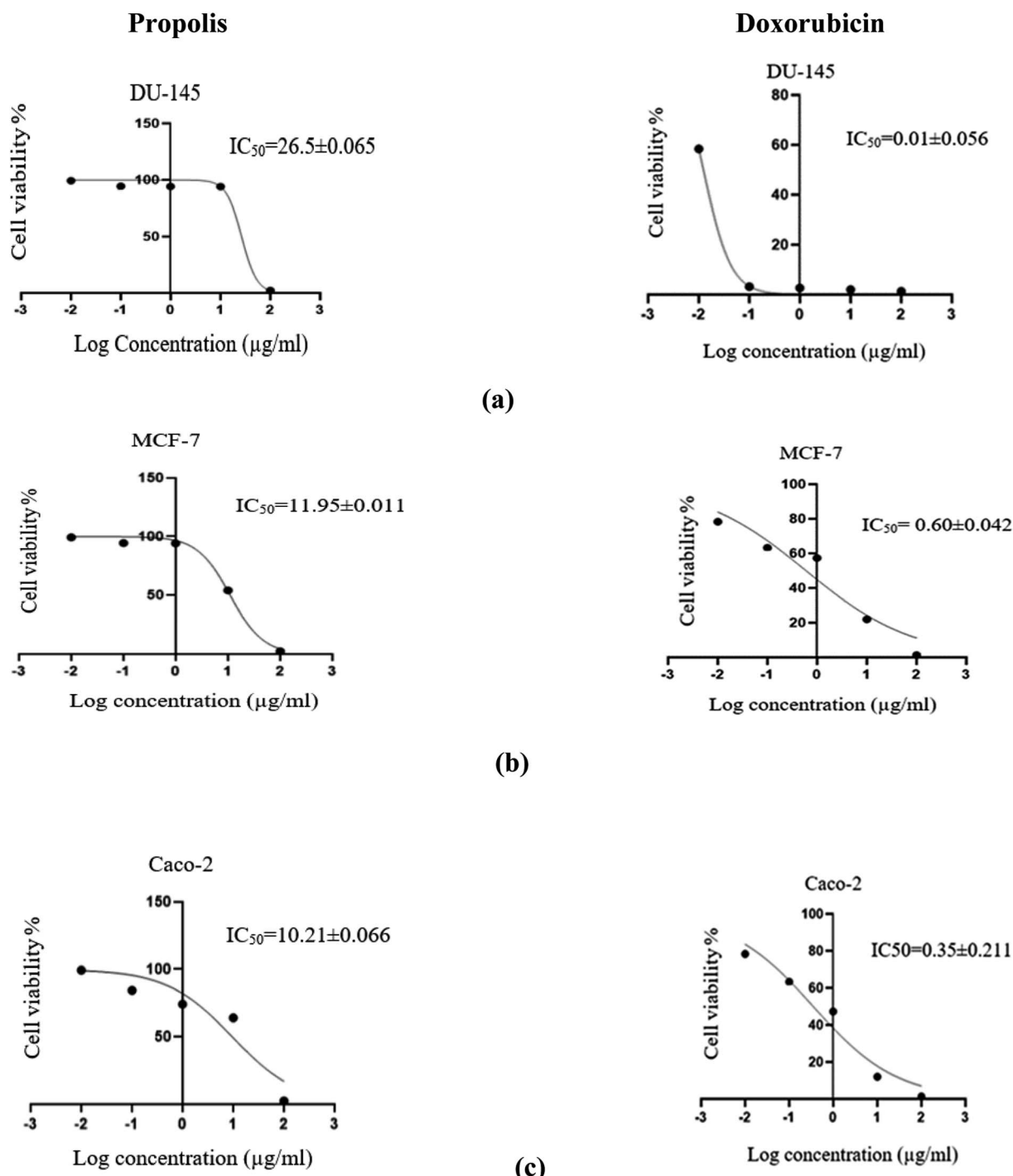


Fig. 10 Dose response curve of propolis extract (to the left) and doxorubicin (to the right) against the human prostate cancer (DU-145) (a), breast adenocarcinoma (MCF-7) (b) and colorectal adenocarcinoma (Caco-2) (c) cell lines.



interactions with Thr62, Thr166 and Thr255 and hydrophobic interaction with Tyr204, Cys170, Phe256, Leu168, Tyr204, Phe256 and Leu168. There was also a charged negative interaction with Glu167⁴⁸ (Fig. 8C).

Whereas, the stabilization of quercetin interaction with RAC-alpha serine/threonine-protein kinase (PDB ID 3O96) was through the formation of four hydrogen bonds between 5, 7, 3' and 4' hydroxyl groups and Gln79, Thr211 and Ser205, and a pi-pi stacking interaction between the aromatic ring A of the flavone moiety and Trp80. There were also polar interactions with Thr81, Thr82 and Asn54 and hydrophobic interactions with Tyr263, Leu264, Ile84, Val270, Tyr272, Leu210, Ala212, and Ile290. In addition to positively charged interaction with Lys268 and negatively charged interaction with Asp292⁴⁹ (Fig. 9A).

On the other hand, the interaction of genistein with aromatase (PDB ID 3EQM) involved four hydrogen bonds between 5, 7, 3' and 4' hydroxyl groups and Ala 306, Leu477, Leu372 and Met374 residues. There were also hydrophobic interactions with Phe134, Ile133, Ala307, Trp224, Phe221, Val370 and Val 373 and polar interaction with Ser478 and Thr310. In addition to a charged positive interaction with Arg115^{50,51} (Fig. 9B). While the interaction of genistein with endothelial nitric oxide synthase (PDB ID 1M9K) was stabilized *via* the formation of a hydrogen bond between 4' hydroxyl group and Ser354 and a pi-pi stacking interaction between the aromatic ring A of the flavone moiety and Trp178. In addition to the formation of coordination reaction with Hem901 and hydrophobic interactions with Leu193, Ala227, Ile228, Phe353, Phe473, Ala181, Met339, Trp447, Cys184. There were also a charged positive interaction with Arg183 and polar interaction with Ser226⁵² (Fig. 9C).

3.5. *In vitro* anticancer activity of propolis extract on human prostate (DU-145), breast (MCF-7) and colorectal (Caco-2) cancer cell lines

The propolis extract was subjected to *in vitro* anticancer activity testing on human prostate (DU-145), breast (MCF-7) and colorectal (Caco-2) cancer cell lines. The results shown in Fig. 10 indicated the high propolis potency against the studied cancer types, where it showed IC₅₀ values equal to 26.5 ± 0.06, 11.95 ± 0.01 and 10.213 ± 0.07 µg mL⁻¹ in human prostate (DU-145), breast (MCF-7) and colorectal (Caco-2) cancer cell lines, respectively. These results are concordant with the literature survey summarized in Table 3 demonstrating the activity of propolis constituents against the studied cancer cell lines where luteolin was found to induce G2/M cell-cycle arrest in human colon cancer cell lines.⁵³ Whereas quercetin was reported to suppress viability and proliferation of MCF-7 cells by activation of both apoptosis and necroptosis signaling pathways.⁵⁴ It was also found to exert anticancer effect on DU-145 cells by modulating ROS, Akt, and NF-κB pathways.⁵⁵ The Egyptian propolis extract exhibited more potent cytotoxic activity than well-known cytotoxic agents such as platinum nanocatalysts⁵⁶ and even propolis from other regions such as Moroccan and Indian propolis.^{57,58} DAVID pathway analysis of prostate (Fig. S1†), breast (Fig. S2†) and colorectal (Fig. S3†) cancer illustrates the

potential targets and pathways of Egyptian propolis chemical constituents. The red ovals indicate the targets where the molecules interact and the pink rectangles indicate the targeted pathways.

4. Conclusion

Due to the complex metabolome of natural products and the high cost of in-laboratory screening of their role and mechanism of action in various diseases, the network pharmacology-based analysis is regarded as a valuable mean to accomplish this task easily and more conveniently. In this study, the network pharmacology-based analysis of propolis showed that the hit propolis constituents related to cancer targets were genistein, luteolin, benzoic acid, quercetin and vanillic acid. Whereas, the main cancer-associated targets were CYP1A1, CYP19A1, ESR1, NOS3, CASP3 and AKT1. Twenty-four cancer-related pathways were recognized where the most enriched ones were pathways in cancer and estrogen signaling pathway. Among hit compounds, molecular docking studies revealed that quercetin had the lowest binding energy with cytochrome P450 1A1, estrogen receptor, caspase-3 and RAC-alpha serine/threonine-protein kinase. Whereas, genistein exhibited the most stabilized interaction with aromatase and endothelial nitric oxide synthase. This study represents a thorough explanation of the proposed mechanism of action of propolis constituents in cancer and suggests this natural product as a potential source of phytoconstituents that can be implemented for cancer prevention or treatment. Further extensive *in vivo* and clinical studies are required to confirm the anti-cancer potential of the concluded top hit natural compounds.

Conflicts of interest

There are no conflicts to declare.

References

- WHO, *Preventing chronic diseases: a vital investment*, https://www.who.int/chp/chronic_disease_report/en/, accessed February 16, 2021.
- S. F. Sener and N. Grey, *J. Surg. Oncol.*, 2005, **92**, 1–3.
- C. D. Mathers and D. Loncar, *PLoS Med.*, 2006, **3**, e442.
- A. G. Desai, G. N. Qazi, R. K. Ganju, M. El-Tamer, J. Singh, A. K. Saxena, Y. S. Bedi, S. C. Taneja and H. K. Bhat, *Curr. Drug Metab.*, 2008, **9**, 581–591.
- S. I. Anjum, A. Ullah, K. A. Khan, M. Attaullah, H. Khan, H. Ali, M. A. Bashir, M. Tahir, M. J. Ansari, H. A. Ghramh, N. Adgaba and C. K. Dash, *Saudi J. Biol. Sci.*, 2019, **26**, 1695–1703.
- S. Patel, *J. Diet. Suppl.*, 2016, **13**, 245–268.
- V. Bankova, M. Popova and B. Trusheva, *Phytochemistry*, 2018, **155**, 1–11.
- V. C. Toreti, H. H. Sato, G. M. Pastore and Y. K. Park, *J. Evidence-Based Complementary Altern. Med.*, 2013, **2013**, 1–13.
- M. Shahinuzzaman, N. Taira, T. Ishii, M. Halim, M. Hossain and S. Tawata, *Molecules*, 2018, **23**, 2479.



10 C. Meneghelli, L. S. D. Joaquim, G. L. Q. Félix, A. Somensi, M. Tomazzoli, D. A. da Silva, F. V. Berti, M. B. R. Veleirinho, D. d. O. S. Recouvreux, A. C. de Mattos Zeri, P. F. Dias and M. Maraschin, *Microvasc. Res.*, 2013, **88**, 1–11.

11 B. Gogoi, D. Gogoi, Y. Silla, B. B. Kakoti and B. S. Bhau, *Mol. BioSyst.*, 2017, **13**, 406–416.

12 M. Liao, H. Shang, Y. Li, T. Li, M. Wang, Y. Zheng, W. Hou and C. Liu, *Phytomedicine*, 2018, **45**, 93–104.

13 J. Ma, J. Huang, S. Hua, Y. Zhang, Y. Zhang, T. Li, L. Dong, Q. Gao and X. Fu, *J. Ethnopharmacol.*, 2019, **231**, 152–169.

14 A. S. P. Pereira, M. J. Bester and Z. Apostolides, *Mol. Diversity*, 2017, **21**, 809–820.

15 A. Upadhyay, P. Agrahari and D. K. Singh, *Int. J. Pharmacol.*, 2014, **10**, 289–298.

16 A. L. Hopkins, *Nat. Chem. Biol.*, 2008, **4**, 682–690.

17 C. A. Lipinski, *Drug Discovery Today: Technol.*, 2004, **1**, 337–341.

18 X.-Q. Shi, S.-J. Yue, Y.-P. Tang, Y.-Y. Chen, G.-S. Zhou, J. Zhang, Z.-H. Zhu, P. Liu and J.-A. Duan, *J. Ethnopharmacol.*, 2019, **235**, 227–242.

19 U. Chandran and B. Patwardhan, *J. Ethnopharmacol.*, 2017, **197**, 250–256.

20 E. Shawky, A. A. Nada and R. S. Ibrahim, *RSC Adv.*, 2020, **10**, 27961–27983.

21 M. Hong, Y. Zhang, S. Li, H. Y. Tan, N. Wang, S. Mu, X. Hao and Y. Feng, *Molecules*, 2017, **22**, 1–11.

22 H. M. Dawood, R. S. Ibrahim, E. Shawky, H. M. Hammada and A. M. Metwally, *J. Ethnopharmacol.*, 2018, **224**, 359–372.

23 L. Kubiliene, V. Laugaliene, A. Pavilonis, A. Maruska, D. Majiene, K. Barcauskaite, R. Kubilius, G. Kasparaviciene and A. Savickas, *BMC Complementary Altern. Med.*, 2015, **15**, 1–7.

24 R. M. Allam, A. M. Al-Abd, A. Khedr, O. A. Sharaf, S. M. Nofal, A. E. Khalifa, H. A. Mosli and A. B. Abdel-Naim, *Toxicol. Lett.*, 2018, **291**, 77–85.

25 P. Skehan, R. Storeng, D. Scudiero, A. Monks, J. McMahon, D. Vistica, J. T. Warren, H. Bokesch, S. Kenney and M. R. Boyd, *J. Natl. Cancer Inst.*, 1990, **82**, 1107–1112.

26 H. Tang, S. He, X. Zhang, S. Luo, B. Zhang, X. Duan, Z. Zhang, W. Wang, Y. Wang and Y. Sun, *J. Evidence-Based Complementary Altern. Med.*, 2016, **2016**, 1–10.

27 M. Kuhn, C. von Mering, M. Campillos, L. J. Jensen and P. Bork, *Nucleic Acids Res.*, 2008, **36**, D684–D688.

28 R. Apweiler, A. Bairoch, C. H. Wu, W. C. Barker, B. Boeckmann, S. Ferro, E. Gasteiger, H. Huang, R. Lopez, M. Magrane, M. J. Martin, D. A. Natale, C. O'Donovan, N. Redaschi and L. S. L. Yeh, *Nucleic Acids Res.*, 2017, **45**, D158–D169.

29 H. M. Naif, M. A. I. Al-Obaide, H. H. Hassani, A. S. Hamdan and Z. S. Kalaf, *Frontiers in Public Health*, 2018, **6**, 1–7.

30 J. R. Long, N. Kataoka, X. O. Shu, W. Wen, Y. T. Gao, Q. Cai and W. Zheng, *Cancer Epidemiol., Biomarkers Prev.*, 2006, **15**, 2115–2122.

31 C. Thomas and J. Å. Gustafsson, *Nat. Rev. Cancer*, 2011, **11**, 597–608.

32 L. Ying and L. J. Hofseth, *Cancer Res.*, 2007, **67**, 1407–1410.

33 N. O'donovan, J. Crown, H. Stunell, A. D. K. Hill, E. Mcdermott, N. O'higgins, M. J. Duffy and S. Vincent', *Clin. Cancer Res.*, 2003, **9**, 738–742.

34 M. Song, A. M. Bode, Z. Dong and M. H. Lee, *Cancer Res.*, 2019, **79**, 1019–1031.

35 M. Kanehisa and S. Goto, *Nucleic Acids Res.*, 2000, **28**, 27–30.

36 Y. Li, F. Ahmed, S. Ali, P. A. Philip, O. Kucuk and F. H. Sarkar, *Cancer Res.*, 2005, **65**, 6934–6942.

37 D. Y. Lim, H. J. Cho, J. Kim, C. W. Nho, K. W. Lee and J. H. Y. Park, *BMC Gastroenterol.*, 2012, **12**, 1–10.

38 J. Girouard, D. Belgorosky, J. Hamelin-Morissette, V. Boulanger, E. D'orio, D. Ramla, R. Perron, L. Charpentier, C. van Themsche, A. M. Eiján, G. Bérubé and C. Reyes-Moreno, *Biochem. Pharmacol.*, 2020, **176**, 1–15.

39 L. Khorsandi, M. Orazizadeh, F. Niazvand, M. R. Abbaspour, E. Mansouri and A. Khodadadi, *Bratislava Medical Journal*, 2017, **118**, 123–128.

40 J. Gong, S. Zhou and S. Yang, *Int. J. Mol. Sci.*, 2019, **20**, 1–18.

41 M. Ashburner, C. A. Ball, J. A. Blake, D. Botstein, H. Butler, J. M. Cherry, A. P. Davis, K. Dolinski, S. S. Dwight, J. T. Eppig, M. A. Harris, D. P. Hill, L. Issel-Tarver, A. Kasarskis, S. Lewis, J. C. Matese, J. E. Richardson, M. Ringwald, G. M. Rubin and G. Sherlock, *Nat. Genet.*, 2000, **25**, 25–29.

42 G. Dennis Jr, B. T. Sherman, D. A. Hosack, J. Yang, W. Gao, H. C. Lane and R. A. Lempicki, *Genome Biol.*, 2003, **4**, R60.1–R60.11.

43 B. D. Green, A. M. Jabbour, J. J. Sandow, C. D. Riffkin, D. Masouras, C. P. Daunt, M. Salmanidis, G. Brumatti, B. A. Hemmings, M. A. Guthridge, R. B. Pearson and P. G. Ekert, *Cell Death Differ.*, 2013, **20**, 1341–1349.

44 A. G. Porter and R. U. Jänicke, *Cell Death Differ.*, 1999, **6**, 99–104.

45 J. Chang, L. Hong, Y. Liu, Y. Pan, H. Yang, W. Ye, K. Xu, Z. Li and S. Zhang, *Cancer Manage. Res.*, 2020, **12**, 2641–2651.

46 V. P. Androutsopoulos, A. Papakyriakou, D. Vourloumis, A. M. Tsatsakis and D. A. Spandidos, *Pharmacol. Ther.*, 2010, **126**, 9–20.

47 N. v. Puranik, P. Srivastava, G. Bhatt, D. J. S. John Mary, A. M. Limaye and J. Sivaraman, *Sci. Rep.*, 2019, **9**, 1–11.

48 B. Muthukala, K. Sivakumari and K. Ashok, *Int. J. Curr. Pharm. Res.*, 2015, **7**, 13–16.

49 X. Bai, Y. Tang, Q. Li, Y. Chen, D. Liu, G. Liu, X. Fan, R. Ma, S. Wang, L. Li, K. Zhou, Y. Zheng and Z. Liu, *Sci. Rep.*, 2021, **11**, 1–25.

50 M. van Dijk, A. M. ter Laak, J. rg D. Wichard, L. Capoferri, N. P. E. Vermeulen and D. P. Geerke, *J. Chem. Inf. Model.*, 2017, **57**, 2294–2308.

51 E. D. Lephart, *Enzyme Res.*, 2015, **2**, 1–11.

52 H. Si, J. Yu, H. Jiang, H. Lum and D. Liu, *Endocrinology*, 2012, **153**, 3190–3198.

53 W. Wang, P. C. VanAlstyne, K. A. Irons, S. Chen, J. W. Stewart and D. F. Birt, *Nutr. Cancer*, 2004, **48**, 106–114.

54 L. Khorsandi, M. Orazizadeh, F. Niazvand, M. R. Abbaspour, E. Mansouri and A. Khodadadi, *Bratislava Medical Journal*, 2017, **118**, 123–128.



55 A. B. Ward, H. Mir, N. Kapur, D. N. Gales, P. P. Carriere and S. Singh, *World Journal of Surgical Oncology*, 2018, **16**, 1–12.

56 P. G. González-Larraza, T. M. López-Goerne, F. J. Padilla-Godínez, M. A. González-López, A. Hamdan-Partida and E. Gómez, *ACS Omega*, 2020, **5**, 25381–25389.

57 S. Touzani, W. Embaslat, H. Imtara, A. Kmail, S. Kadan, H. Zaid, I. Elarabi, L. Badiaa, B. Saad and Y. Kabir, *BioMed Res. Int.*, 2019, 1–11.

58 M. K. Choudhari, R. Haghniaz, J. M. Rajwade and K. M. Paknikar, *Evidence-Based Complementary and Alternative Medicine*, 2013, pp. 1–10.

